

## Porous nanocomposites of zirconium dioxide and silicate†

H. Y. Zhu,\*<sup>a</sup> Z. P. Hao<sup>a</sup> and J. C. Barry<sup>b</sup><sup>a</sup> Department of Chemical Engineering, The University of Queensland, St. Lucia, Qld 4072, Australia.

E-mail: hyzhu@cheque.uq.edu.au; Fax: 61 7 33654199; Tel: 61 7 3365905

<sup>b</sup> Centre of Microanalysis and Microscopy, The University of Queensland, St. Lucia, Qld 4072, Australia

Received (in Cambridge, UK) 8th August 2002, Accepted 4th October 2002

First published as an Advance Article on the web 29th October 2002

**Highly porous nanocomposites of zirconium dioxide and silicate are synthesised in an aqueous system from an inorganic salt of zirconium; the nanocomposites, with tailorable pore structures, exhibit superior performance as catalyst supports.**

Zirconium dioxide (ZrO<sub>2</sub>) is a very attractive material as catalyst or catalyst supports and solid-state electrolyte for fuel cells.<sup>1–3</sup> The large specific surface area of ZrO<sub>2</sub> often leads to superior catalytic activities. However, the synthesis of pure ZrO<sub>2</sub> with large surface areas appears to be complicated, involving templated synthesis methodology, careful choices of surfactant as template and a zirconium precursor normally in non-aqueous systems.<sup>4,5</sup> Electrodeposition can also be used to prepare ZrO<sub>2</sub>. Here we report the synthesis of thermally stable, mesoporous composite nanostructures of fine ZrO<sub>2</sub> and silicate particles. In such a structure the silicate can be regarded as the medium which allows ZrO<sub>2</sub> to be dispersed as stable nanoparticles. Therefore, a large surface area of ZrO<sub>2</sub> is available for the catalytically active component as well as the reactant molecules.

The precursors of the ZrO<sub>2</sub> particles are polymerised cations of zirconium hydroxide, which can be prepared readily from inorganic salts. A synthetic layered clay, laponite, was used as the silicate source. An obvious advantage of this synthesis is that the particles can be prepared in aqueous systems through simple procedures, similar to the synthesis of ZrO<sub>2</sub> pillared clays. However, ZrO<sub>2</sub> pillared clays are microporous solids of only moderate porosity,<sup>6</sup> in which it is difficult to alter the size of the pillars or the pore structure of the pillared clays so limiting their applications.

Laponite has a smectite clay structure. In a dilute aqueous dispersion the clay exists as discrete plates of 20–30 nm in diameter.<sup>7</sup> Therefore, this clay is an ideal inorganic medium to form nanometer-scale composite structures with zirconium hydroxy species. We also found that introducing polyethylene oxide (PEO) surfactants with a general chemical formula C<sub>12–14</sub>H<sub>25–29</sub>O(CH<sub>2</sub>CH<sub>2</sub>O)<sub>n</sub>H (*n* = 5–30) to the clay dispersion can greatly increase the porosity of the resultant composite.

In general, an aqueous ZrOCl<sub>2</sub> solution was refluxed for a few hours and used as a precursor for ZrO<sub>2</sub>, which contains zirconium hydroxyl oligomers.<sup>6</sup> This solution (pH ≈ 1) was added into a suspension of the clay and PEO, which was made by dispersing laponite in deionized water under stirring, and the PEO surfactant was added to this dispersion with continuous stirring. The obtained mixture had a pH of about 9–10 and was aged at 373 K for two days. The solid was recovered from the mixture by centrifuging and was washed with deionized water. The wet cake was dried in air and calcined at 773 K for 20 h.

The surfactants also have a function of separating the precursor species of ZrO<sub>2</sub> particles, preventing them from further condensation and sintering during the drying and calcination processes. During heating the precursors are subjected to dehydration and converted to ZrO<sub>2</sub> particles, and

the surfactant evaporates at above 473 K, leaving a rigid nanostructure with high porosity. To examine the effect of the properties of the surfactants on the structure of ZrO<sub>2</sub>-nanocomposite solids, samples were prepared using different surfactants as well as with the same surfactant but in various surfactant to clay ratios (PEO/Clay ratio). The BET specific surface area (obtained from the Brunauer–Emmett–Teller equation) and porosity data of some nanocomposite samples are listed in Table 1.

In Table 1, *n* indicates the number of the –(CH<sub>2</sub>CH<sub>2</sub>O)– groups in the PEO surfactant. Thus, the molecules of a PEO surfactant with a larger *n* value are larger. It is known that the pore size of the product is closely related to the molecular size of the surfactant in the templated synthesis.<sup>8</sup> The micelles of quaternary ammonium surfactants are uniform cylindrical rods and the diameter of the rods is proportional to the molecular size of the surfactants. However, with the use of the PEO surfactants, the trend appears quite different in this study. The pore volume, mean pore size and even the specific surface area, of the samples decrease with *n*, and thus the molecular size. This could be due to the stronger interaction with the precursor surface for the surfactant with large *n*. Besides, the amount of a PEO surfactant introduced into the synthesis can greatly influence the pore structure. The BET surface area of the samples increases with the PEO/Clay ratio first, reaching a maximum at a ratio at 3.0 and then decreasing with further increase in ratio. Interestingly, we found that incorporating a small quantity of CeO<sub>2</sub> (see Table 2) results in remarkable increases in surface area and pore volume (Table 1). This finding suggests that use of a binary oxide is an additional effective means to create nanocomposites of large porosity. The pore volume and pore size of these nanocomposites is much larger than those of ZrO<sub>2</sub>-pillared clays (0.2–0.3 cm<sup>3</sup> g<sup>–1</sup> and 200–300 m<sup>2</sup> g<sup>–1</sup>).<sup>6</sup>

The pore size distribution (PSD) of ZrO<sub>2</sub>-nanocomposites can be derived from nitrogen adsorption data (Fig. S1, ESI†). The PSDs of the nanocomposite peak at about 4 nm, almost three times of the pore size as in conventional ZrO<sub>2</sub> pillared clays (about 1.4 nm).<sup>6</sup> Considering that the laponite dispersion has a high pH between 9.5 and 10, such a high pH value inevitably induces the further hydrolysis of zirconium oligomer

**Table 1** BET specific surface area, pore volume and mean hydraulic diameter of the framework pores in ZrO<sub>2</sub> nanocomposite samples

Surfactant	<i>S</i> <sub>BET</sub> /m <sup>2</sup> g <sup>–1</sup>	<i>V</i> <sub>p</sub> /cm <sup>3</sup> g <sup>–1</sup>	<i>d</i> <sub>p</sub> /nm
<i>n</i> = 5	437	0.765	7.0
<i>n</i> = 7	428	0.592	5.5
<i>n</i> = 9	459	0.430	3.9
<i>n</i> = 12	340	0.405	4.8
<i>n</i> = 30	300	0.335	4.5
PEO/Clay ratio ( <i>n</i> = 9)			
0	211	0.174	3.3
0.5	401	0.401	4.0
1.0	391	0.360	3.6
2.0	459	0.430	3.9
3.0	465	0.406	3.6
5.0	304	0.377	4.4
CeO <sub>2</sub> /ZrO <sub>2</sub> -nanocomposite ( <i>n</i> = 9)			
2.0	611	0.674	4.4

† Electronic supplementary information (ESI) available: Fig. S1: pore size distributions (PSD) of the calcined ZrO<sub>2</sub>-nanocomposites. See <http://www.rsc.org/suppdata/cc/b2/b207779p/>

**Table 2** Major chemical composition of some nanocomposite samples

Sample	PEO/Clay ratio	SiO <sub>2</sub> (%)	Al <sub>2</sub> O <sub>3</sub> (%)	MgO (%)	Na <sub>2</sub> O (%)	ZrO <sub>2</sub> (%)	CeO <sub>2</sub> (%)
Laponite Nanocomposite	0	51.1	0.1	23.2	2.51	— <sup>a</sup>	—
ZrO <sub>2</sub> -laponite-0	0	33.5	0.22	0.68	—	41.9	—
ZrO <sub>2</sub> -laponite-2	2	41.0	0.20	4.6	—	33.7	—
ZrO <sub>2</sub> -laponite-3	3	40.3	0.25	4.5	—	34.4	—
CeO <sub>2</sub> /ZrO <sub>2</sub> -laponite-2	2	43.9	0.24	3.8	—	35.5	0.54

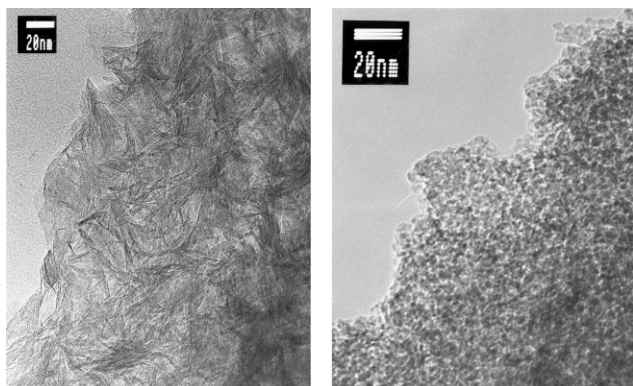
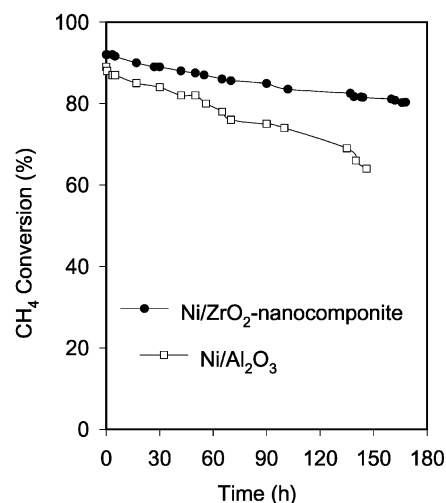
<sup>a</sup> Not detectable.

ions when the precursor solution is introduced. These will condense on the silicate fragments that are products of acid leaching of the laponite platelets, resulting in composite structures with large pore size. The silicate also has a function of stabilising the ZrO<sub>2</sub> nanoparticles, preventing them from sintering during the heating process.

In this work, we did not observe a clear peak in the X-ray diffraction (XRD) patterns of the resultant nanocomposite samples. This suggests that the structures of these solids lack long-range order, and are different from the intercalated structure of pillared clays, which can be examined by the *d*<sub>001</sub> peak in their XRD patterns.<sup>6</sup>

Transmission electron microscopy (TEM) images of the pristine laponite and a ZrO<sub>2</sub>-nanocomposite (with *n* = 7, PEO/Clay ratio = 3, as a representative) are shown in Fig. 1. Bundles of several clay platelets can be seen in the image of pristine laponite in Fig. 1(a). They aggregate in a poor long-range order; while the clay layers can not be seen in the TEM images of the ZrO<sub>2</sub>-nanocomposite sample, there are a large number of ZrO<sub>2</sub> grains with a size of several nanometers. The results of *in-situ* elemental analysis by energy dispersive X-ray spectroscopy (EDXS) also support this composite nanostructure. The chemical composition at several regions of a sample, randomly chosen, was found to be consistent with the overall composition of the sample. The smallest region measured is about 15 nm in diameter, which demonstrates that the uniform composition is due to a composite structure on the nanometer scale. The MgO content in the nanocomposite sample is obviously smaller, compared with that in the pristine laponite. The lower content implies possible Mg leaching during the synthesis by the precursor solution of zirconium, which is acidic. Acid leaching of clays occurs under moderate conditions,<sup>9</sup> leaving small silicate fragments in the product solids.

In the last two decades, application of pillared clays as catalysts or catalyst supports for numerous chemical reactions has been attempted.<sup>10</sup> In general, larger specific surface area, pore volume and pore size as well as high acidity are required for catalysis. Based on these properties, the ZrO<sub>2</sub>- and CeO<sub>2</sub>/ZrO<sub>2</sub>-nanocomposites reported in this study are remarkably superior to the conventional ZrO<sub>2</sub>-pillared clays and they are of great potential for these catalytic applications. In our study, ZrO<sub>2</sub>-composites were used as supports to prepare supported nickel catalysts for methane reforming with carbon dioxide. As

**Fig. 1** TEM images of the starting clay laponite (a) and a calcined ZrO<sub>2</sub>-nanocomposite sample (b).**Fig. 2** Performance of nickel catalysts on a nanocomposite and on activated alumina for methane reforming with carbon. (Reaction conditions: CH<sub>4</sub>/CO<sub>2</sub> = 1 : 1, *P* = 1 atm and flow rate = 60 ml min<sup>-1</sup>).

illustrated in Fig. 2, the catalysts supported on ZrO<sub>2</sub> nanocomposites exhibited high conversion and good stability, maintaining high activity for over 170 h at 1023 K. By contrast, a nickel catalyst on a conventional activated Al<sub>2</sub>O<sub>3</sub> support showed substantial deactivation.

These findings highlight the potential of the ZrO<sub>2</sub> nanocomposites as advanced materials. These solids can be readily granulated to designed shapes and the grains have good mechanical strength because of the presence of silicate nanoparticles.

In addition, the synthesis strategy for constructing nanocomposites with a large porosity and tailorable structure in aqueous systems, which we proposed in this study, could be applied to synthesise nanocomposites of other metal oxides and other layered clays. Such studies are being conducted.

Financial support from the Australian Research Council (ARC) is gratefully acknowledged. H. Y. Z. is indebted to ARC for the QE II fellowship. Thanks also to Ms X. Yan for conducting part of the experimental work.

## Notes and references

- 1 J. A. Lercher, J. H. Bitter, W. Hally, W. Niessen and K. Seshan, *Stud. Surf. Sci. Catal.*, 1996, **101**, 463.
- 2 J. M. Wei, B. Q. Xu, J. L. Li, Z. X. Cheng and Q. M. Zhu, *Appl. Catal. A.*, 2000, **196**, 167L.
- 3 X. S. Li, J. S. Chang and S. E. Park, *React. Kinet. Catal. Lett.*, 1999, **67**, 375.
- 4 J. A. Knowles and M. J. Hudson, *J. Chem. Soc., Chem. Commun.*, 1995, 2083.
- 5 P. Yang, D. Zhao, D. I. Margolese, B. F. Chmelka and G. D. Stucky, *Nature*, 1998, **396**, 152.
- 6 K. Ohtsuka, Y. Hayashi and M. Suda, *Chem Mater.*, 1993, **5**, 1823.
- 7 D. W. Thompson and J. T. Butterworth, *J. Colloid Interface Sci.*, 1992, **151**(1), 236.
- 8 C. T. Kresge, M. E. Leonowicz, W. J. Roth, J. C. Vartuli and J. S. Beck, *Nature*, 1992, **359**, 710.
- 9 R. Mokaya and W. Jones, *J. Catal.*, 1995, **153**(1), 76.
- 10 A. Gil, L. M. Gandia and M. A. Vicente, *Catal. Rev.*, 2000, **42**(1/2), 145.